# Fibroblast adhesion on unidirectional polymeric nanofilms

Christof Christophis
*Applied Physical Chemistry, University of Heidelberg, 69120 Heidelberg, Germany*

Koray Sekeroglu and Gokhan Demirel
*Materials Research Institute and Department of Engineering Science, The Pennsylvania State University, University Park, Pennsylvania 16802*

Isabel Thome and Michael Grunze
*Applied Physical Chemistry, University of Heidelberg, 69120 Heidelberg, Germany and Institute of Functional Interfaces, IFG, Karlsruhe Institute of Technology, PO Box 3640, 76021 Karlsruhe, Germany*

Melik C. Demirel[a)]
*Materials Research Institute and Department of Engineering Science, The Pennsylvania State University, University Park, Pennsylvania 16802*

Axel Rosenhahn[a)]
*Applied Physical Chemistry, University of Heidelberg, 69120 Heidelberg, Germany and Institute of Functional Interfaces, IFG, Karlsruhe Institute of Technology, PO Box 3640, 76021 Karlsruhe, Germany*

(Received 2 August 2011; accepted 14 September 2011; published 7 October 2011)

Nanotextured polymeric surfaces with inclined rods reveal highly anisotropic properties concerning wetting and adhesion. In this work, we report on the interaction of fibroblast cells with these highly anisotropic materials. The authors quantified removal of adherent cells from such surfaces by a laminar flow. The critical shear force needed for cell removal from the surface depends on the inclination direction. Based on electron microscopy cross sections we deduce that interactions of cellular filopodia extending into the nanotextured surface are causing the direction depending removal. © *2011 American Vacuum Society*. [DOI: 10.1116/1.3646093]

## I. INTRODUCTION

Cell adhesion is an important phenomenon in many fundamental processes such as angiogenesis, cancer cell metastasis, and wound healing.[1–3] Cell adhesion on surfaces has been studied extensively using various *in vitro* techniques including micromanipulation techniques (e.g., micropipette aspiration, laser trapping), MEMS tools (e.g., micropillar arrays, microcantilever sensors), and microfabrication approaches (e.g., ECM micropatterning, microfluidic shear devices, micro/nano-substrates, traction force microscopy).[4–6] A number of studies have focused on microfluidic devices to investigate the effect of shear on cells to understand its relevance for physiological processes and to reveal biophysical properties of cells.[7–10] These microchannels require minimal sample volume and are easy to fabricate that makes them attractive for high throughput screening and biomedical studies.[11,12] Simple approaches of modifying the surface properties of microfluidic channels[13] while maintaining their mechanical properties are desirable for a range of cell culture applications, "organ-on-a-chip" devices[14] or the mimicking of blood flows to investigate metabolic mechanisms.[15] Our group applied microfluidics to quantify attachment strength and revealed the influence of hydration on fibroblast cell adhesion[16] and rolling and adhesion of hematopoietic progenitor cells on hyalurons.[17]

Besides chemistry, morphology and especially morphologies on the nanoscale were found to be highly relevant for cell adhesion. Nanostructured biomaterials (e.g., polymers, ceramics, metals) promote specific interactions and functions with proteins and cells.[18] For example, nanotextured titanium enhances cell adhesion and osseointegration.[19,20] It has been also shown that nanoscale roughness of polymeric scaffolds enhanced the adhesion and proliferation of bladder urothelial cells.[21] Cell adhesion studies on RGD-functionalized gold nanoparticles revealed that cell adhesion depends on both, the spacing and the geometric arrangement of nanoparticles.[22–24] Recently, Demirel *et al.*[25–27] synthesized bioinspired unidirectional surfaces for precisely tuning surface physicochemical properties. These surfaces, which comprise an asymmetric array of tilted nanorods, can transport water droplets in fluidic channels,[28] provide directional adhesion,[29] and exhibit directional friction.[30]

So far it is unknown if anisotropies on the nanoscale affect cell adhesion. Here we report fibroblast adhesion assays in a microfluidic device coated with a unidirectional polymeric nanofilm. Specifically, we studied the directional removal of fibroblast cells from tilted poly(p-chloro-xylylene) nanorods (nanoPPX) by a hydrodynamic shear force, and quantified the influence of flow direction with respect to nanorod tilting orientation on the critical shear stress needed for cell removal. A laminar flow in a microfluidic device was applied in different directions relative to the nanorod tilting (Fig. 1). Rat embryonic fibroblasts (REF52) were selected for the cell adhesion strength assay on nanoPPX substrates as a model cell line.[16]

[a)]Authors to whom correspondence should be addressed; electronic addresses: mdemirel@engr.psu.edu; axel.rosenhahn@kit.edu

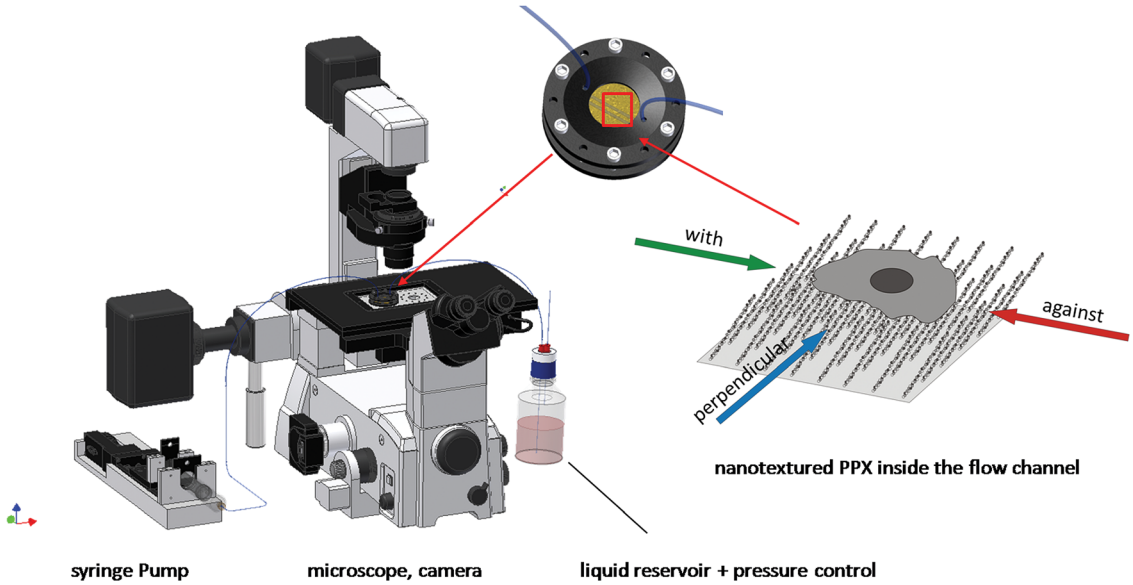


FIG. 1. (Color online) Scheme of the microfluidic shear force assay for probing cell adhesion. The liquid flow has been applied "with" (green), "perpendicular" (blue), or "against" (red) the tilting of the nanoPPX-film.

## II. MATERIALS AND METHODS

### A. Preparation of nanoPPX-films on glass

A polished glass slide has been cleaned by successive immersions in $HCl/CH_3OH$ (1:1 v/v), deionized water, and concentrated $H_2SO_4$. Afterwards styrylethyltrimethoxysilane (Gelest, PA, USA) was used to form a self-assembled organosilane monolayer to enhance the adherence of the poly (p-chloro-xylylene) (PPX-Cl) film to the glass substrate.[31] The substrate was baked on a hotplate at 120 °C for 4 min to complete the dehydration reaction that forms the siloxane bond between the organosilane and the glass substrate. PPX-Cl deposition was performed using a Parylene Deposition System PDS 2010 (SCS, Indianapolis, IN, USA) modified by using a glass bell jar (BOC Edwards, Wilmington, MA, USA) as vacuum chamber and a nozzle for directing the flow.[32–34] Source material, (2,2)-dichloroparacyclophane in powder form (Uniglobe-Kisco, Whiteplains, NY, USA), was heated to produce a directed vapor flux onto a substrate through the nozzle. The relative angle between the vapor flux and the substrate was varied by tilting the substrate. Deposition was performed at vapor-flux angles $\alpha$ of 10° with respect to the substrate surface resulting in columnar thin-film coatings of tilt angles $\beta$ (i.e., 57°–63°). Planar films were deposited by operating the coating system in normal configuration using a baffle to disperse the entering PPX-Cl vapor. Deposition parameters such as sublimation temperature, pyrolysis temperature and chamber vacuum were kept the same for both the planar and columnar film deposition; these values were set to 175 °C, 690 °C, and 32 Torr, respectively.

### B. Cell culture

The cell adhesion strength on nanoPPX was evaluated *in vitro* using rat embryonic fibroblast cells (REF52), which serves as well characterized[35] model cell line from the connective tissue especially suited for cell adhesion studies. The cells were cultured in a humidified incubator with 5% $CO_2$ at 37 °C. The culture medium was Dulbecco's modified Eagle's Medium (DMEM) supplemented with 10% fetal bovine serum, 1 mM L-glutamine, and 100 units per mL penicillin–streptomycin solution all purchased from Gibco (Invitrogen, Karlsruhe, Germany). The cells were harvested from tissue culture flasks by incubation with a 0.05% trypsin–EDTA solution for 5 min. Cells were rinsed with medium, resuspended in DMEM and diluted to $4 \times 10^5$ cells per mL before injection into the channel system.

### C. Microfluidic cell detachment assay

A custom built microfluidic setup was used as described in detail recently.[16] In brief, the setup comprises an incubator housed inverted microscope and a parallelized channel system as major components. The channel (25.0 mm × 1.5 mm × 145 $\mu$m) is situated between a glass channel and the nanoPPX coated glass substrate. The shear stress along the channel walls generated by a liquid flow can be described according to Poiseuille's model[36] with Eq. (1). The one-dimensional approximation is justified as the width of the channels is much larger than the height ($w > 10h$). The wall shear stress $\tau$, referred to as shear stress, depends on the volumetric flow rate $Q$, the viscosity of the fluid $\mu$ ($\sim 0.72 \times 10^{-3}$ kg m$^{-1}$ s$^{-1}$ for cell medium at 37 °C[37]) and the channel dimensions height $h$ and width $w$. This simple model agrees with 3D numerical calculations[7] and with literature following the Purday approximation:[37]

$$\tau = \frac{6Q\mu}{h^2 w}. \quad (1)$$

The flow was controlled by a custom built syringe pump at the channel outlet. For the cell detachment assay the flow

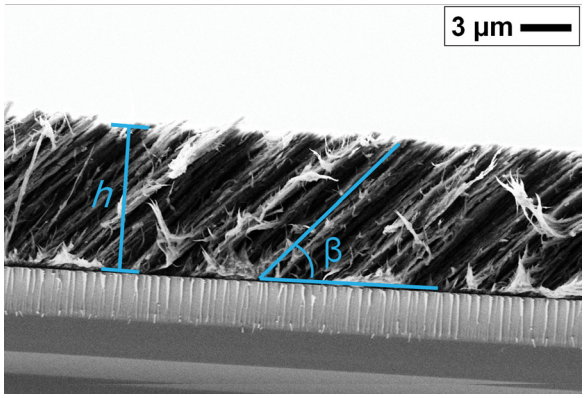


FIG. 2. (Color online) SEM image of a cross section PPX-film on glass substrate. Nanorod tilting angle $\beta$ and PPX film height $h$ were measured for all surfaces.

was raised every 5 s by 26% to probe the wall shear stress over 5 orders of magnitude. The maximum shear stress exerted in this experiment can be as high as 3000 dyn $cm^{-2}$, values high enough to remove even well spread cells. The fraction of adherent cells has been determined by time lapse microscopy during flow exposure every 5 s and the fraction of attached cells was plotted against a logarithmic shear stress scale.[16] The critical shear stress $\tau_{50}$ is defined as the removal of 50% of adherent cell population.[38] The video microscopy images and subsequent SEM images did not show major residual cell parts, which indicates that the cells are rather removed from the surface than ruptured.[39]

### D. Sample Characterization

NanoPPX films have been characterized by using a scanning electron microscope (SEM) LEO 1530 (Zeiss, Oberkochen, Germany) after the experiments (Fig. 2). The substrates were sputtered with carbon and imaged at 3 keV electron energy and a working distance of 3–4 mm using secondary electron (SE) and backscattered electron (BE) detectors. Column tilt angles and film thicknesses were measured using the NIS-Elements software (Nikon, Tokyo, Japan). Cross sections reveal the mean film height to be $h = 7.0 \pm 0.5$ $\mu$m and the tilting angle $\beta = 57°$–$63°$ which is close to the theoretical expectation of 55° (for $\alpha = 10°$) according to the empirical formula in Eq. (2), where $\beta$ and $\alpha$ are the column and deposition tilt angles, respectively:[40]

$$\tan(\beta) = 0.5 \tan(\alpha). \quad (2)$$

For electron micrographs, adherent fibroblasts on nanoPPX were fixed and critical point dried. Therefore, fibroblast cells were incubated in supplemented DMEM on nanoPPX for 5 h. The substrates were washed with phosphate buffered saline (PBS) and then incubated with 2% paraformaldehyde in PBS for 15 min at room temperature. After fixation, substrates were washed with PBS solution and PBS was exchanged for MilliQ water in three steps. Subsequently, the water was substituted by abs. ethanol in six steps (10 min each), starting with 50% ethanol. Finally samples were immersed two times in 100% abs. ethanol for 1 h to remove remaining water traces. The substrates were transferred into a critical point dryer (CPD 030, Bal-Tec, Schalksmühle, Germany) and ethanol was exchanged by $CO_2$. Subsequently, the $CO_2$ was evaporated in the overcritical phase. Prior to SEM, the substrates were sputtered with carbon to render the surface conductive.

Figure 3 shows the optical transparency of the nanoPPX films. Transmission measurements are done using the Varian Cary UV-Vis spectrophotometer. All measurements are made from 300 to 800 nm. The spectral bandwidth of the beam is 2 nm and the scanning rate is 600 nm/min. Oscillating data is typically observed for planar thin films. NanoPPX

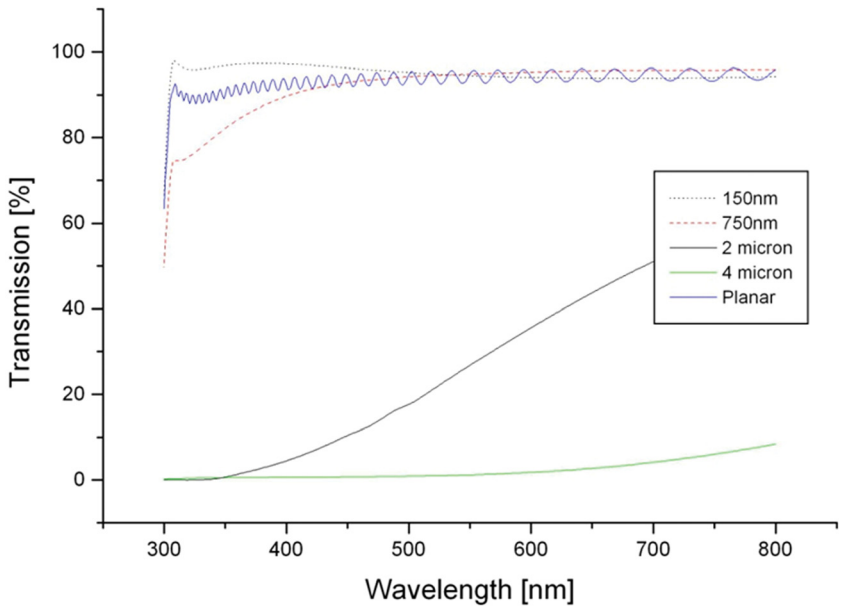


FIG. 3. (Color online) Optical transparency of nanoPPX films with various thicknesses (150 nm to 4 $\mu$m) are shown. Transparency of planar-PPX film (oscillating data) is also provided for comparison.

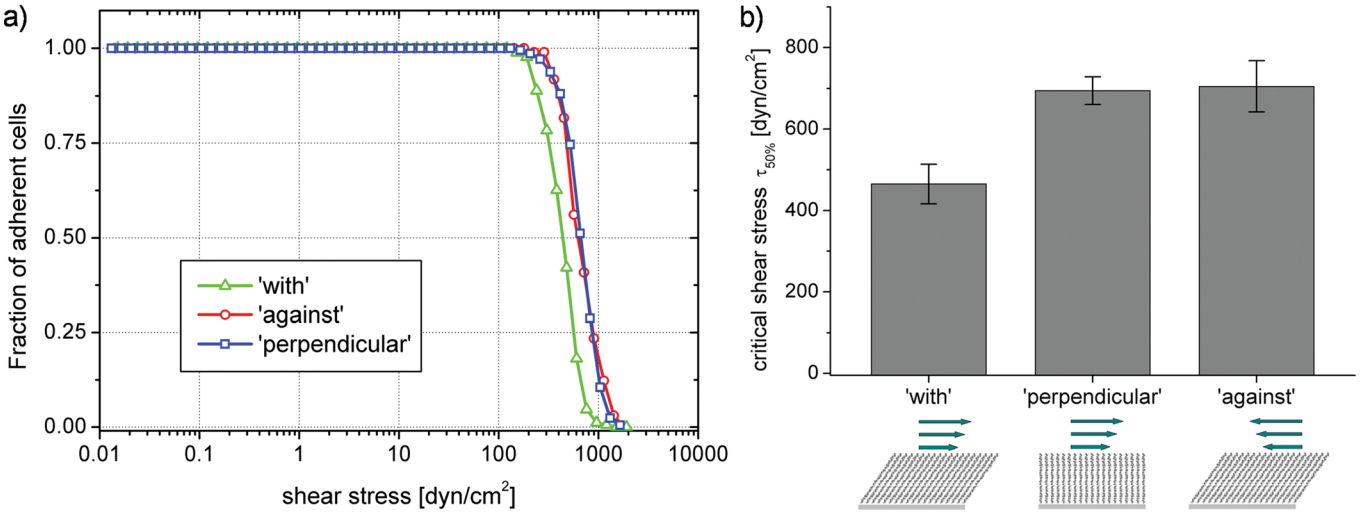


FIG. 4. (Color online) (a) Exemplary detachment curve for fibroblast adhesion strength on nanoPPX films. The adhesion strength was higher if the flow has been applied against (circles) and perpendicular (squares) with respect to the tilting direction of PPX-films then for flow with the tilting direction (triangles). (b) Critical shear stress required to remove REF52 fibroblasts from nanoPPX films for the different flow directions. Values represent the average of four independent experiments, error bars are the standard error.

films become opaque in the visible region as the thickness of the film increases.

## III. RESULTS AND DISCUSSION

### A. Flow direction depending removal of cells from nano-PPX

NanoPPX substrates were mounted in the microfluidic channel in three orientations with respect to the applied shear stress (i.e., with, against, and perpendicular). REF52 fibroblasts were harvested from cell culture plates, and injected into the channel. The cells were incubated on nanoPPX films for 5 h inside the three microchannels. Towards the end of the incubation phase, the morphology of the cells appeared to be well spread, as found on a reference glass substrate in a fourth channel. Afterwards the microfluidic shear force assay for ~250 cells in each channel was carried out. Therefore, the flow has gradually been increased every 5 seconds by 26% according to our recently published protocol.[16] The decreasing number of adherent cells was recorded over time as function of the applied shear force [Fig. 4(a)]. The weakest adherent fibroblasts were removed from the nanoPPX surface at shear forces exceeding 100 dyn/cm$^2$ [Fig. 4(a)]. In order to obtain sufficient statistics, the critical shear stress was determined by four independent experiments for each tilting direction. The analysis revealed that cells were removed at higher critical shear stress if the flow was applied "against" and "perpendicular" with respect to the tilting direction (705 ± 63 dyn/cm$^2$ and 695 ± 34 dyn/cm$^2$, respectively), but at much lower shear force "with" tilting direction (465 ± 48 dyn/cm$^2$) [Fig. 4(b)]. The absolute values are characteristic for a surface which allows the cells to adhere rather strongly. For comparison, the critical shear stress needed for removal of fibroblasts

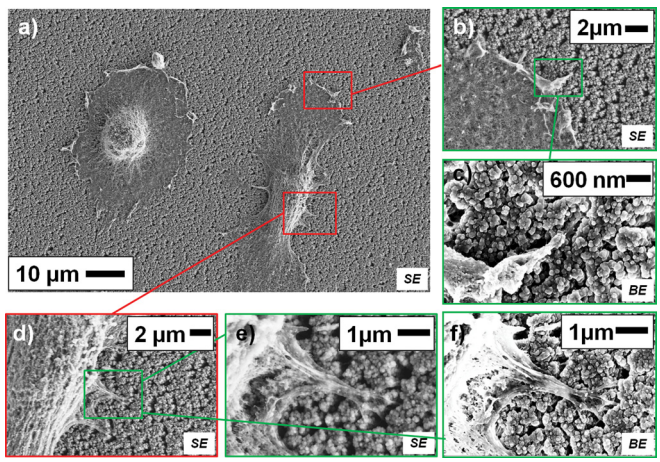


FIG. 5. (Color online) Top view SEM images of REF52 fibroblasts attached to the nanoPPX substrate. Cell filopodia show attachment into the holes between the nanorods at high magnifications.

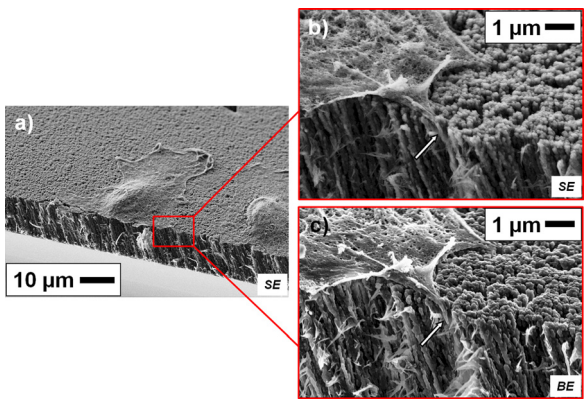


FIG. 6. (Color online) SEM image of REF52 fibroblasts at the edge of a cut nanoPPX substrate. The surface was tilted by 45° with respect to normal incidence of the electron beam (a). High magnification images (b, c) show cell filopodia (arrow) penetrating ~0.5 µm deep into the holes. The SEM images in (b) and (c) were recorded with the secondary electron and the backscattering detector, respectively.

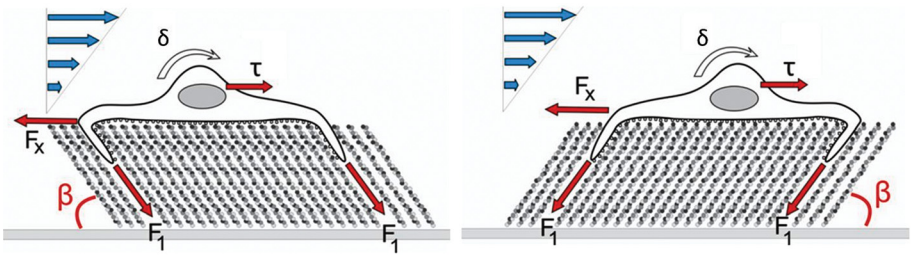


FIG. 7. (Color online) Sketch of cell filopodia attaching in between the tilted nanoPPX-film. The angle between anchoring force $F_1$ and hydrodynamic shear $\tau$ varies depending on the flow direction. $F_x$ denotes the adhesion force and $\delta$ the torque due to the flow.

from a fibrinogen or collagen coated glass slide is in the order of 1000 dyn/cm$^2$ or higher,[41] from an uncoated glass slide in the order of 700 dyn/cm$^2$ (Refs. 16 and 41), and from a self-assembled monolayer with three ethylene glycol units in the order of 3 dyn/cm$^2$ (very weak adhesion).[16]

### B. Electron micrographs of adherent cells on nanoPPX

In order to understand the observed differences in cell removal, we investigated the shape and the spreading process of the cells by optical, fluorescence and electron microscopy in greater detail. The opaque nature of the nanostructured polymer (Fig. 3) hampered light and fluorescent microscopy, and it was not possible to obtain images, which allowed drawing mechanistic conclusions on focal contacts or attachment of filopodiae. Therefore, we restricted morphological analysis of the adherent fibroblasts on nanoPPX to scanning electron microscopy. SEM images revealed the cell morphology in greater detail (Fig. 5). Most of the cells were well spread and established filopodiae at their periphery comparable to the adhesion on glass. Also, no obvious distortion of cell orientation or shape due to the anisotropy of the substrate was detected. Images at higher magnification revealed that some of the peripheral filopodiae penetrate into the randomly distributed defects between the nanorods.

The isotropic cell spreading on nanoPPX films indicates that cells do not actively respond to the anisotropic surface, e.g., by unidirectional elongation. Recently, tribology experiments[30] on nanoPPX surfaces revealed that sliding forces across the surface exhibit also a directional dependence. In these measurements, the indenter tip is forced perpendicular to the surface while recording the force required moving it laterally. The mechanical response to sliding was studied relative to the film structural anisotropy by examining contact friction and deformation in three sliding orientations: "with," "against," and "perpendicular" to the tilt axis of the columns. Friction coefficients were uniformly high (0.5–1.5) for all orientations. Neither frictional anisotropy nor depth hysteresis was observed for sliding perpendicular to the column tilt axis. However, sliding with and against the column tilt axis resulted in measurable friction anisotropy as well as depth hysteresis, with larger contact depths and higher friction coefficients for sliding with the column tilt. Our experiments indicate that such asymmetric sliding resistance has no obvious effect on the cell spreading process.

Tilted cross section SEM images show that the filopodiae are anchored in the substrate as they were able to penetrate in between the nanorods (Fig. 6). The filopodiae reach up to 0.5 $\mu$m inside the substrate between the nanorods. This leads to a possible explanation for the increased capability of the cells to withstand the fluid shear stress when flow is applied against or perpendicular to the tilting direction of the PPX nanorods. The applied flow exerted a shear stress parallel to the substrate, either with anchoring direction or against it as sketched in Fig. 7. The directionality of anchoring could be one reason for the reduced critical shear stress necessary to remove the cells, as the filaments can easier be pulled out of the surface when the shear force is applied with the direction along nanorod tilting. The force balance can be described by Laufenburger's dynamic model for cell adhesion,[42] which predicts removal once the applied shear stress $\tau$ exceeds the counteracting adhesion force $F_x$. $F_x$ denotes the adhesion force of the filaments if removed parallel to the nanorods $F_1$ (Fig. 7). As the shear stress $\tau$ is applied perpendicular to the surface, the inclination angle of the nanorods $\beta$ causes a different geometric situation for the anchoring filopodiae, depending in which direction the shear is applied. As a consequence, both, the torque $\delta$ and the bending modulus of the filaments over the top of the rods will contribute to the force balance parallel to the surface and ultimately lead to a different geometric equilibrium condition for the critical shear stress for removal along the two tilting directions.

## IV. SUMMARY AND CONCLUSIONS

We demonstrated that cell adhesion on a directional surface in the form of nanorods leads to an anisotropic removal behavior in our microfluidic attachment strength assay. Cross section micrographs suggest that filopodia penetrating in between the polymer rods are responsible for the anisotropic removal. The different force contributions were discussed on the basis of Laufenburger's dynamic model of adhesion. Future research will focus on the effect of inclination angle, chemistry and mechanical stiffness on directional cell adhesion and correlation with cytoskeletal processes.

## ACKNOWLEDGMENTS

The authors thank the Sander Stiftung (Proposal 2010.079.1), the Office of Naval research (Grant number N00014-08-1-1116), the Pennsylvania State University, and

the Helmholtz program Biointerfaces for support of this work. The authors thank Geert Schmid-Schonbein (UCSD) for a number of useful discussions and kindly acknowledge the support of the cell culture team of Spatz (Heidelberg University and MPI for metal research, Stuttgart).

[1]P. C. Brooks, R. A. F. Clark, and D. A. Cheresh, Science **264**, 569 (1994).
[2]C. S. Chen, M. Mrksich, S. Huang, G. M. Whitesides, and D. E. Ingber, Science **276**, 1425 (1997).
[3]P. Martin, Science **276**, 75 (1997).
[4]M. Dembo and Y. L. Wang, Biophys. J. **76**, 2307 (1999).
[5]D. H. Kim, P. K. Wong, J. Park, A. Levchenko and Y. Sun, Ann. Rev. Biomed. Eng. **11**, 203 (2009).
[6]E. W. K. Young and C. A. Simmons, Lab Chip **10**, 143 (2009).
[7]H. Lu, L. Y. Koo, W. C. M. Wang, D. A. Lauffenburger, L. G. Griffith, and K. F. Jensen, Anal. Chem. **76**, 5257 (2004).
[8]N. Korin, A. Bransky, U. Dinnar and S. Levenberg, Lab Chip **7**, 611 (2007).
[9]B. Lincoln, F. Wottawah, S. Schinkinger, S. Ebert and J. Guck, Cell Mech. **83**, 397 (2007).
[10]N. Walter, A. Micoulet, T. Seufferlein and J. P. Spatz, Biointerphases **6**, 117 (2011).
[11]A. Manbachi, S. Shrivastava, M. Cioffi, B. G. Chung, M. Moretti, U. Demirci, M. Yliperttula and A. Khademhosseini, Lab Chip **8**, 747 (2008).
[12]S. Moon, S. K. Hasan, Y. S. Song, F. Xu, H. O. Keles, F. Manzur, S. Mikkilineni, J. W. Hong, J. Nagatomi, E. Haeggstrom, A. Khademhosseini and U. Demirci, Tissue Eng. Part C **16**, 157 (2010).
[13]L. Bocquet and J. L. Barrat, Soft Matter **3**, 685 (2007).
[14]S. R. Khetani and S. N. Bhatia, Nat. Biotechnol. **26**, 120 (2008).
[15]G. W. Schmid-Schonbein, Physiol. Rev. **70**, 987 (1990).
[16]C. Christophis, M. Grunze and A. Rosenhahn, Phys. Chem. Chem. Phys. **12**, 4498 (2010).
[17]C. Christophis, I. Taubert, G. R. Meseck, M. Schubert, M. Grunze, A. D. Ho, and A. Rosenhahn, Biophys. J. **101**, 585 (2011).
[18]M. Goldberg, R. Langer, and X. Jia, J. Biomater. Sci. **18**, 241 (2007).
[19]D. Khang, J. Lu, C. Yao, K. M. Haberstroh, and T. J. Webster, Biomaterials **29**, 970 (2008).
[20]A. J. Dulgar-Tulloch, R. Bizios, and R. W. Siegel, J. Biomed. Mater. Res. Part A **90**, 586 (2009).
[21]Y. W. Chun, D. Khang, K. M. Haberstroh, and T. J. Webster, Nanotechnology **20**, (2009).
[22]M. Arnold, E. A. Cavalcanti-Adam, R. Glass, J. Blummel, W. Eck, M. Kantlehner, H. Kessler, and J. P. Spatz, Chemphyschem **5**, 383 (2004).
[23]E. A. Cavalcanti-Adam, M. Bezler, P. Tomakidi, and J. P. Spatz, J. Bone Miner. Res. **19**, S64 (2004).
[24]E. A. Cavalcanti-Adam, A. Micoulet, J. Blummel, J. Auernheimer, H. Kessler, and J. P. Spatz, Eur. J. Cell Biol. **85**, 219 (2006).
[25]M. Cetinkaya, S. Boduroglu, and M. C. Demirel, Polymer **48**, 4130 (2007).
[26]M. C. Demirel, S. Boduroglu, M. Cetinkaya, and A. Lakhtakia, Langmuir **23**, 5861 (2007).
[27]M. C. Demirel, Colloids and Surf. **321**, 121 (2008).
[28]N. A. Malvadkar, M. J. Hancock, K. Sekeroglu, W. J. Dressick, and M. C. Demirel, Nat. Mater. **9**, 1023 (2010).
[29]S. Boduroglu, M. Cetinkaya, W. J. Dressick, A. Singh, and M. C. Demirel, Langmuir **23**, 11391 (2007).
[30]E. So, M. C. Demirel, and K. J. Wahl, J. Phys. D **43**, 045403 (2010).
[31]M. C. Demirel, M. Cetinkaya, A. Singh, and W. J. Dressick, Adv. Mater. **19**, 4495 (2007).
[32]M. Cetinkaya, N. Malvadkar, and M. C. Demirel, J. Polym. Sci., Part B: Polym. Phys. **46**, 640 (2008).
[33]M. Cetinkaya and M. C. Demirel, Chem. Vap. Deposition **15**, 101 (2009).
[34]G. Demirel, N. Malvadkar, and M. C. Demirel, Thin Solid Films **518**, 4252 (2010).
[35]J. I. Garrels and B. R. Franza, J. Biol. Chem. **264**, 5283 (1989).
[36]W. M. Deen, *Analysis of Transport Phenomena* (Oxford University Press, New York, 1998).
[37]E. W. K. Young, A. R. Wheeler, and C. A. Simmons, Lab Chip **7**, 1759 (2007).
[38]A. J. Garcia, P. Ducheyne, and D. Boettiger, Biomaterials **18**, 1091 (1997).
[39]B. P. Chan, A. Chilkoti, W. M. Reichert, and G. A. Truskey, Biomaterials **24**, 559 (2003).
[40]J. M. Nieuwenhuizen and H. B. Haanstra, Philips Tech. Rev. **27**, 87 (1966).
[41]K. Christ, K. Williamson, K. Masters, and K. Turner, Biomed. Microdevices **12**, 443 (2010).
[42]D. A. Hammer and D. A. Lauffenburger, Biophys. J. **52**, 475 (1987).